LEARNING VALUE FUNCTIONS FROM UNDIRECTED STATE-ONLY EXPERIENCE

Anonymous authors
Paper under double-blind review

ABSTRACT

This paper tackles the problem of learning value functions from undirected state-only experience (state transitions without action labels *i.e.* (s, s', r) tuples). We first theoretically characterize the applicability of Q-learning in this setting. We show that tabular Q-learning in discrete Markov decision processes (MDPs) learns the same value function under any arbitrary refinement of the action space. This theoretical result motivates the design of Latent Action Q-learning or LAQ, an offline RL method that can learn effective value functions from state-only experience. Latent Action Q-learning (LAQ) learns value functions using Q-learning on discrete latent actions obtained through a latent-variable future prediction model. We show that LAQ can recover value functions that have high correlation with value functions learned using ground truth actions. Value functions learned using LAQ lead to sample efficient acquisition of goal-directed behavior, can be used with domain-specific low-level controllers, and facilitate transfer across embodiments. Our experiments in 5 environments ranging from 2D grid world to 3D visual navigation in realistic environments demonstrate the benefits of LAQ over simpler alternatives, imitation learning oracles, and competing methods.

1 INTRODUCTION

Offline or batch reinforcement learning focuses on learning goal-directed behavior from pre-recorded data of undirected experience in the form of (s_t, a_t, s_{t+1}, r_t) quadruples. However, in many realistic applications, action information is not naturally available (*e.g.* when learning from video demonstrations), or worse still, isn't even well-defined (*e.g.* when learning from the experience of an agent with a different embodiment). Motivated by such use cases, this paper studies if, and how, intelligent behavior can be derived from undirected streams of observations: (s_t, s_{t+1}, r_t).[1]

At the face of it, it might seem that observation-only data would be useless towards learning goal-directed policies. After all, to learn such a policy, we need to know what actions to execute. If those are simply missing from the dataset then nothing can be done. Our key conceptual insight is that while an observation-only dataset doesn't tell us the precise action to execute, *i.e.* the policy $\pi(a|s)$; it may still tell us which states are more likely to lead us to the goal than not, *i.e.* the value function $V(s)$. For example, simply by looking at someone working in the kitchen, we can infer that approaching the microwave handle is more useful (*i.e.* has higher value) for opening the microwave than to approach the buttons. Thus, we can still make use of observation-only data, if we focused on learning value functions as opposed to directly learning goal-directed policies. Once we have learned a good value function, it can be used to quickly acquire or infer behavior. Using learned value functions as dense rewards can lead to quick policy learning through some small amount of interaction in the environment. Alternatively, they could be used to directly guide the behavior of low-level controllers that may already be available for the agent (as is often the case in robotics) without any further training. Furthermore, decoupling the learning of value functions from policy learning enables deriving behavior for agents with a different embodiment as long as the overall strategy to solve the task remains similar.

Thus, the central technical question is how to learn a good value function from undirected observation streams. Is it even possible? If so, under what conditions? This paper tackles these questions from a theoretical and practical perspective.

[1] We assume r_t is observed. Reward can often be sparsely labeled in observation streams with low effort.

We start out by characterizing the behavior of tabular Q-learning from Watkins (1989) under missing action labels. We note that Q-learning without action labels amounts to policy evaluation, *i.e.*, the learned value function estimates the value of the implicit policy that generated the observation stream. Thus, depending on the policy that generated the data, the learned values (without any action grounding) can differ from the optimal values. Furthermore, it is possible to construct simple environments where the behavior implied by the learned value function is also sub-optimal.

Next, we present a more optimistic result. There are settings in which Q-learning can recover the optimal value function even in the absence of the knowledge of underlying actions. Concretely, we prove that if we are able to obtain an action space which is a strict refinement of the original action space, then Q-learning in this refined action space recovers the optimal value function.

This motivates a practical algorithm for learning value functions from the given undirected observation-only experience. We design a latent-variable future prediction model that seeks to obtain a refined action space. It operates by predicting s_{t+1} from s_t and a discrete latent variable $\hat{a}$ from a set of actions $\hat{\mathbf{A}}$ (Section 4.1). Training this latent variable model assigns a discrete action $\hat{a}_t$ to each (s_t, s_{t+1}) tuple. This allows us to employ Q-learning to learn good value functions (Section 4.2). The learned value function is used to derive behavior (Section 4.3) either through some online interaction with the environment, or through the use of domain specific low-level controllers.

Our experiments in five environments (2D grid world, 2D continuous control, Atari game Freeway, robotic manipulation, and visual navigation in realistic 3D environments) test our proposed ideas. Our method approximates a refinement of the latent space better than clustering alternatives, and in turn, learns value functions highly correlated with ground truth. Good value functions in-turn lead to sample efficient acquisition of behavior, leading to significant improvement over learning with only environment rewards. Our method compares well against existing methods that learn from undirected observation-only data, while being also applicable to the case of high-dimensional observation spaces in the form of RGB images. We are also able to outperform imitation learning methods, even when these imitation learning methods have access to privileged ground-truth action information. Furthermore, our method is able to use observation-only experience from one agent to speed up learning for another agent with a different embodiment. Code, models, simulation environments will be released.

2 Preliminaries

Following the notation from Sutton & Barto (2018), our Markov decision process (MDP) is specified by $(\mathbf{S}, \mathbf{A}, p, \gamma)$, where $\mathbf{S}$ is a state space, $\mathbf{A}$ is an action space, γ is the discount factor, and $p(s', r|s, a)$ is the state/reward joint dynamics function. It specifies the probability distribution that the agent ends up in state s', receives a reward of r on executing action a from state s.

Offline or batch RL (Lange et al., 2012; Levine et al., 2020) studies the problem of deriving high reward behavior when only given a dataset of experience in an MDP, in the form of a collection of quadruples (s, a, s', r). In this paper, we tackle a harder version of this problem where instead we are only given a collection of triplets (s, s', r), *i.e.* experience without information about intervening actions. In general, this dataset could contain any quality of behavior, from optimal, to actively adversarial. In contrast to some methods (see Section 7), we will not assume that demonstrations in the dataset are of high quality, and design our method to be robust to sub-optimal data.

In this paper, we will focus on methods based on Q-learning (Watkins, 1989) for tackling this problem. Q-learning has the advantage of being *off-policy*, *i.e.*, experience from another policy (or task) can be used to learn or improve a different policy for a different task. Q-learning seeks to learn the optimal Q-function $Q^*(s, a)$ by iteratively updating $Q(s_t, a_t)$ to the bellman equation. This process converges to the Q^* under mild conditions in many settings (Watkins, 1989).

3 Characterizing Q-learning without True Action Labels

We characterize the outcome of Q-learning in settings where we don't have ground truth intervening actions in the offline dataset being used for Q-learning. We first consider the case of ignoring the action altogether, which amounts to TD(0) policy evaluation. Next, we study if labeling (s, s', r)

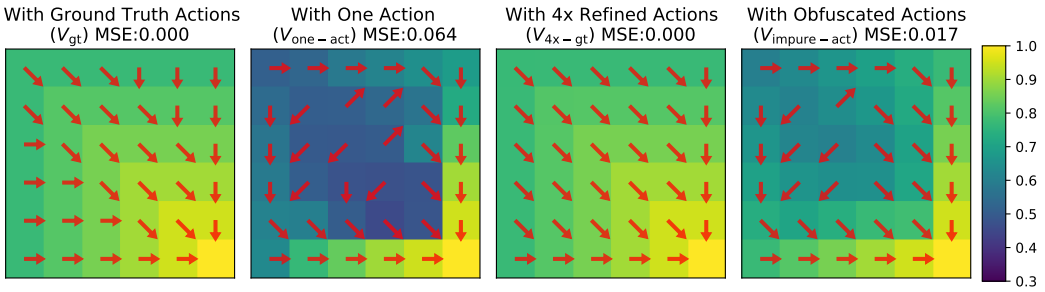

Figure 1: We visualize the learned value function when using different action labels for Q-learning: ground truth actions, one single action, a $4\times$ refined action space, and obfuscated actions. We also report the mean squared error from the optimal value function. Arrows show the behavior induced by the value function (picking neighboring state with highest value). See Section 3.2 for more details.

samples with actions from a different action space $\hat{\mathbf{A}}$ to construct a new MDP could aid learning. More specifically, can the optimal Q-function for this new MDP, as obtained through Q-learning on samples (s, s', r) labeled with actions from $\hat{\mathbf{A}}$, be useful in the original MDP? We show that under the right conditions the value function learned under the altered action space $\hat{\mathbf{A}}$ is identical to the value function learned for the original MDP.

Q-learning with no action labels (single action): Without action labels, one could simply assign all transitions the same label. In this case, Q-Learning becomes TD(0) policy evaluation. The induced value function isn't the optimal value function for the MDP, but rather the value according to the policy that generated the dataset. Depending on the dataset, this could be sub-optimal.

3.1 Optimality of Action Refinement

Assume we have a Markov Decision Process (MDP) M specified by $(\mathbf{S}, \mathbf{A}, p, \gamma)$. Let the action space $\mathbf{A}$ be composed of actions $a_1, a_2, a_3, ..., a_n \in \mathbf{A}$. We are interested in the value learned under a modified MDP, $\hat{M}$ composed of $(\mathbf{S}, \hat{\mathbf{A}}, \hat{p}, \gamma)$. We will show that if the actions and transitions $\hat{\mathbf{A}}$ and $\hat{p}$ are a *refinement* of $\mathbf{A}$ and p, then the value function learned on $\hat{M}$, $V_{\hat{M}}$ is identical to the value function learned on M, V_M. We define actions and transitions in $\hat{M}$ to be a refinement of those in M when, a) in each state, for every action in $\hat{\mathbf{A}}$, there is at least one action in $\mathbf{A}$ which is functionally identical in the same state, and b) in each state, for each action in $\mathbf{A}$ is represented by at least one action in $\hat{\mathbf{A}}$ in that state. Note that this definition of refinement requires a *state conditioned* correspondence between action behavior. Actions do not need to have to correspond across states.

Theorem 3.1. *Given a discrete finite MDP, M specified by $(\mathbf{S}, \mathbf{A}, p)$ and MDP, $\hat{M}$ specified by $(\mathbf{S}, \hat{\mathbf{A}}, \hat{p})$, where*

$$\underset{\hat{a}\in\hat{\mathbf{A}}, s\in\mathbf{S}}{\forall} \; \underset{a\in\mathbf{A}}{\exists} \; \underset{s',r}{\forall} \; \hat{p}(s', r|s, \hat{a}) = p(s', r|s, a), \text{ and } \underset{a\in\mathbf{A}, s\in\mathbf{S}}{\forall} \; \underset{\hat{a}\in\hat{\mathbf{A}}}{\exists} \; \underset{s',r}{\forall} \; \hat{p}(s', r|s, \hat{a}) = p(s', r|s, a),$$

both MDPs learn the same value function, i.e. $\forall_s V^*_{\hat{M}}(s) = V^*_M(s)$.

We prove this by showing that optimal policies under both MDPs induce same value in every state.

Lemma 3.2. *For any policy π_M on M, there exists a policy $\pi_{\hat{M}}$ on $\hat{M}$ such that $V^{\pi_{\hat{M}}}_{\hat{M}}(s) = V^{\pi_M}_M(s)$, $\forall s$, and for any policy $\pi_{\hat{M}}$ on $\hat{M}$ there exists a policy π_M on M such that $V^{\pi_{\hat{M}}}_{\hat{M}}(s) = V^{\pi_M}_M(s)$ $\forall s$.*

We provide proofs for Theorem 3.1 and Lemma 3.2 in Section A.1.

3.2 Gridworld Case Study

We validate these results in a tabular grid world setting. In particular, we measure the error in learned value functions and the induced behavior, when conducting Q-learning with datasets with different qualities of intervening actions. The agent needs to navigate from the top left of a 6×6 grid to the bottom right with sparse reward. We generate data from a fixed, sub-optimal policy

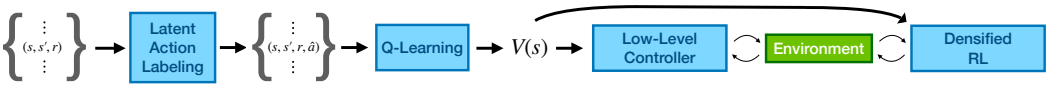

Figure 2: Approach Overview. Our proposed approach Latent Action Q-Learning (LAQ) starts with a dataset of (s, s', r) triples. Using the latent action learning process, each sample is assigned a latent action $\hat{a}$. Q-learning on the dataset of quadruples produces a value function, $V(s)$. Behaviors are derived from the value function through densified RL, or by guiding low-level controllers.

to evaluate all methods in an offline fashion (additional details in Section A.5). We generate 20K episodes with this policy, and obtain value functions using Q-learning under the following 4 choices for the intervening actions: **(1)** Ground truth actions (V_{gt}), **(2)** One action ($V_{\text{one-act}}$, ammounts to TD(0) policy evaluation), **(3)** $4\times$ refinement of original action space ($V_{4\times\text{-gt}}$). We modify the data so that each sample for a particular action in the original action space is randomly mapped to one of 4 actions in the augmented space. **(4)** Obfuscated actions ($V_{\text{impure-act}}$). Original action with probability 0.5, and a random action with probability 0.5.

Figure 1 shows the learned value functions under these different action labels, and reports the MSE from the true value function, along with induced behavior. In line with our expectations, $V_{4\times\text{-gt}}$ which uses a refinement of the actions is able to recover the optimal value function. $V_{\text{one-act}}$ fails to recover the optimal value function, and recovers the value corresponding to the policy that generated the data. $V_{\text{impure-act}}$, under noise in action labels (non-refinement) also fails to recover the optimal value function. Furthermore, the behavior implied by $V_{\text{impure-act}}$ and $V_{\text{one-act}}$ is sub-optimal. We also analyze the effect of the action impurity on learned values and implied behavior. Behavior becomes increasingly inaccurate as action impurity increases. More details in Section A.3.

4 Latent Action Q-Learning

Our analysis in Section 3 motivates the design of our approach for learning behaviors from state-only experience. Our proposed approach decouples learning into three steps: mining *latent* actions from state-only trajectories, using these latent actions for Q-learning to obtain value functions, and learning a policy to act according to the learned value function. As per our analysis, if learned latent actions are a *state-conditioned refinement* of the original actions, Q-learning will result in good value functions, that will lead to good behaviors.

4.1 Latent Actions from Future Prediction

Given a dataset $\mathbf{D}$ of observations streams $\ldots, o_t, o_{t+1}, \ldots$, the goal in this step is to learn *latent* actions that are a refinement of the actual actions that the agent executed. We learn these latent actions through future prediction. We train a future prediction model f_θ, that maps the observation o_t at time t, and a latent action $\hat{a}$ (from a set $\hat{\mathbf{A}}$ of discrete latent actions) to the observation o_{t+1} at time $t+1$, *i.e.* $f_\theta(o_t, \hat{a})$. f is trained to minimize a loss l between the prediction $f_\theta(o_t, \hat{a})$ and the ground truth observation o_{t+1}. $\hat{a}$ is treated as a latent variable during learning. Consequently, f_θ is trained using a form of expectation maximization (Bishop, 2006). Each training sample (o_t, o_{t+1}) is assigned to the action that leads to the lowest loss under the current forward model. The function f_θ is optimized to minimize the loss under the current latent action assignment. More formally, the loss for each sample (o_t, o_{t+1}) is: $L(o_t, o_{t+1}) := \min_{\hat{a}\in\hat{\mathbf{A}}} l\left(f_\theta(o_t, \hat{a}), o_{t+1}\right)$. We minimize $\sum_{(o_t, o_{t+1})\in\mathbf{D}} L(o_t, o_{t+1})$ over the dataset to learn f_θ.

Latent action $\hat{a}_t$ for observation pairs (o_t, o_{t+1}) are obtained from the learned function f_θ as: $\arg\min_{\hat{a}\in\hat{\mathbf{A}}} l\left(f_\theta(o_t, \hat{a}), o_{t+1}\right)$. Choice of the function f_θ and loss l vary depending on the problem. We use L2 loss in the observation space (low-dimensional states, or images).

4.2 Q-learning with Latent Actions

Latent actions mined from Section 4.1 allow us to complete the given (o_t, o_{t+1}, r_t) tuples into $(o_t, \hat{a}_t, o_{t+1}, r_t)$ quadruples for use in Q-learning Watkins (1989). As our actions are discrete we can easily adopt any of the existing Q-learning methods for discrete action spaces (*e.g.* Mnih et al.

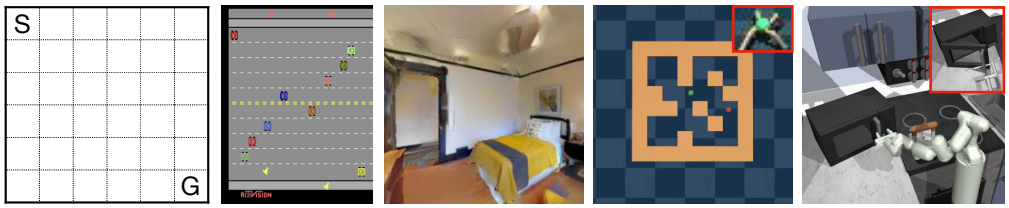

2D Grid World | Freeway | 3D Visual Nav. | 2D Maze | Kitchen

Figure 3: We experiment with five environments: 2D Grid World, Freeway (Atari), 3D Visual Navigation, Maze2D (2D Continuous Control), and FrankaKitchen. Top right corner of Maze2D and FrankaKitchen, shows the embodiments for cross-embodiment transfer (ant and hook, respectively).

(2013)). Though, we note that this Q-learning still needs to be done in an *offline* manner from pre-recorded state-only experience. While we adopt the most basic Q-learning in our experiments, more sophisticated versions that are designed for offline Q-learning (*e.g.* Kumar et al. (2020); Fujimoto et al. (2019)) can be directly adopted, and should improve performance further. Value functions are obtained from the Q-functions as $V(s) = \max_{\hat{a} \in \hat{\mathbf{A}}} Q(s, \hat{a})$.

4.3 Behaviors from Value Functions

Given a value function, our next goal is to derive behaviors from the learned value function. In general, this requires access to the transition function of the underlying MDP. Depending on what assumptions we make, this will be done in the following two ways.

Densified Reinforcement Learning. Learning a value function from state-only experience can be extremely valuable when a dense reward function for the underlying task is not readily available. In this case, using the learned value function can densify sparse reward functions, making previously intractable RL problems solvable. Specifically, we use the value function to create a *potential-based* shaping function $F(s, s') = V(s') - V(s)$, based on Ng et al. (1999), and construct an augmented reward function $r'(s, a, s') = r(s, a, s') + F(s, s')$. Our experiments show that using this densified reward function speeds up behavior acquisition.

Domain Specific Low-level Controllers. In more specific scenarios, it may be possible to employ hand designed low-level controllers in conjunction with a model that can predict the next state s' on executing any of low-level controllers. In such a situation, behavior can directly be obtained by picking the low-level controller that conveys the agent to the state s' that has the highest value under the learned $V(s)$. Such a technique was used by Chang et al. (2020). We show results in their setup.

5 Experiments

We design experiments to assess the quality of value functions learned by LAQ from undirected state-only experience. We do this in 2 ways. First, we measure the extent to which value functions learned with LAQ without ground truth information agree with value functions learned with Q-learning with ground truth action information. This provides a direct quality measure and allows us to compare different ways of arriving at the value function: other methods in the literature (D3G (Edwards et al., 2020)), and simpler alternatives of arriving at latent actions. Our second evaluation measures the effectiveness of LAQ-learned value functions for deriving effective behavior in different settings: when using it as a dense reward, when using it to guide low-level controllers, and when transferring behavior across embodiments. Where possible, we compare to behavior cloning (BC) with *privileged* ground truth actions. BC with ground truth actions serves as an upper bound on the performance of state-only imitation learning methods (BCO from Torabi et al. (2018a), ILPO from Edwards et al. (2019), *etc.*) and allows us to indirectly compare with these methods.

Test Environments. Our experiments are conducted in five varied environments: the grid world environment from Section 3, the Atari game Freeway from Bellemare et al. (2013), 3D visual navigation in realistic environments from Chang et al. (2020); Savva et al. (2019), and two continuous control tasks from Fu et al. (2020)'s D4RL: Maze2D (2D continuous control navigation), and FrankaKitchen (dexterous manipulation in a kitchen). For Maze2D and FrankaKitchen environ-

Table 1: We report Spearman's correlation coefficients for value functions learned using various methods with DQN, against a value function learned offline using ground-truth actions (DQN for discrete action environments, and DDPG for continuous action environments). The *Ground Truth Actions* column shows Spearman's correlation coefficients between two different runs of offline learning with ground-truth actions. See Section 5.1. Details on model selection in Section A.8.

Environment	D3G	Single Action	Clustering	Clustering (Diff)	Latent Actions	Ground Truth Actions
2D Grid World	0.959	0.093	0.430	**1.000**	0.985	1.000
Freeway	– (image input)	0.886	0.945	0.902	**0.961**	0.970
3D Visual Navigation	– (image input)	0.641	0.722	0.827	**0.927**	0.991
2D Continuous Control	0.673	0.673	0.613	0.490	**0.844**	0.851
Kitchen Manipulation	0.854	0.858	0.818	0.815	**0.905**	0.901

ments, we also consider *embodiment transfer*, where we seek to learn policies for an ant and a hook respectively from the observation-only experience of a point mass and the Franka arm. Together, these environments test our approach on different factors that make policy learning hard: continuous control, high-dimensional observations and control, complex real world appearance, 3D geometric reasoning, and learning across embodiments. Environments are visualized in Figure 3, more details about the environments are provided in Section A.4.

Experimental Setup For each setting, we work with a pre-collected dataset of experience in the form of state, next state and reward triplets, (o_t, o_{t+1}, r_t). We use our latent-variable forward model (Section 4.1) and label triplets with latent actions to obtain quadruples $(o_t, \hat{a}_t, o_{t+1}, r)$. We perform Q-learning on these quadruples to obtain value functions $V(s)$, which are used to acquire behaviors either through densified RL by interacting with the environment, or through use of domains-specific low-level controllers. We use the ACME codebase (Hoffman et al., 2020) for experiments.

Latent Action Quality. In line with the theory developed in Section 3, we want to establish how well our method learns a refinement of the underlying action space. To assess this, we study the *state-conditioned purity* of the partition induced by the learned latent actions. Overall, our method is effective at finding refinement of the original action space. It achieves higher state-conditioned purity than a single action, and naive clustering. In high-dimensional image observation settings, it surpasses baselines by a wide margin. Details can be found in Section A.6.

5.1 Quality of Learned Value Functions

We evaluate the quality of the value functions learned through LAQ. We use as reference the value function $V_{\text{gt-act}}$, obtained through *offline* Q-learning (DDPG for continuous action cases) with true ground truth actions *i.e.* (o_t, a_t, o_{t+1}, r_t).[2] For downstream decision making, we only care about the relative ordering of state values. Thus, we measure the Spearman's rank correlation coefficient between the different value functions. Table 1 reports the Spearman's coefficients of value functions obtained using different action labels: single action, clustering, latent actions (ours), and with ground truth actions. We also report Spearman's correlations of value functions produced using D3G (Edwards et al., 2020). In all settings we do Q-learning over the top 8 dominant actions, except for Freeway, where using the top three actions stabilized training.

Our method out performs all baselines in settings with high-dimensional image observations (3D Visual Navigation, Freeway). In state based settings, where clustering state differences is a helpful inductive bias, we see that our method is still on-par with, or superior to clustering state differences and even D3G, which predicts state differences.

5.2 Using Value Functions for Downstream Tasks

Our next experiments test the utility of LAQ-learned value functions for acquiring goal-driven behavior. We first describe the 3 settings that we use to assess this, and then summarize our takeaways.

[2]Offline DDPG in the FrankaKitchen environment was unstable. To obtain a reference value function, we manually define a value function based on the distance between the end-effector and the microwave handle (lower better), and the angle of the microwave door (higher better). We use this as the reference value function.

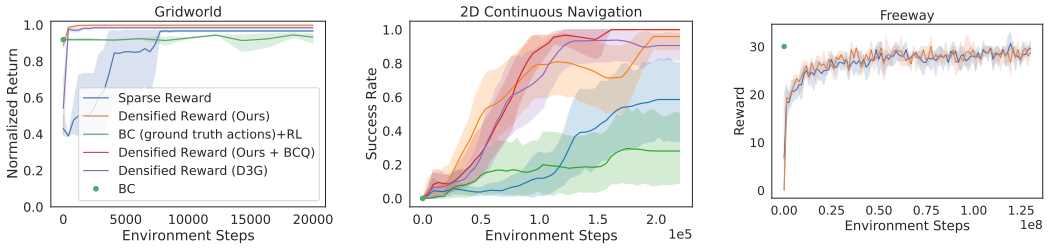

Figure 4: We show learning curves for acquiring behavior using learned value functions. We compare densified RL (Section 4.3) with sparse RL and BC/BC+RL. See Section 5.2 for more details. Results are averaged over 5 seeds and show 95% confidence intervals.

- **Using value functions as dense reward functions**. We combine sparse task reward with the learned value function as a potential function (Section 4.3). We scale up the sparse task rewards by a factor of 5 so that behavior is dominated by the task reward once policy starts solving the task. Figure 4 measures the learning sample efficiency. We compare to only using the sparse reward, behavior cloning (BC) with ground truth actions, and BC followed by spare reward RL.
- **Using value functions to learn behavior of an agent with a different embodiment.** Decoupling the learning of value function and the policy has the advantage that learned value functions can be used to improve learning across embodiment. We demonstrate this, we keep the same task, but change the embodiment of the agent in Maze2D and FrankaKitchen environments. For Maze2D, the point-mass is replaced with a 8-DOF quadrupedal ant. For FrankaKitchen, the Franka arm is replaced with a position-controlled hook. We may need to define how we query the value function when the embodiment (and the underlying state space) changes. For the ant in Maze2D, the location (with 0 velocity) of the ant body is used to query the value function learned with the point-mass. For the hook in FrankaKitchen, the value function is able to transfer directly as both settings observe end-effector position and environment state. We report results in Figure 5.
- **Using value functions to guide low-level controllers.** Learned value functions also have the advantage that they can be used directly at test time to guide the behavior of low-level controllers. We do this experiment in context of 3D visual navigation in a scan of a real building and use the *branching environment* from Chang et al. (2020). We follow their setup and replace their value functions with ones learned using LAQ in their hierarchical policy, and compare the efficiency of behavior encoded by the different value functions.

LAQ value functions speed up downstream learning. Learning plots in Figure 4 show that LAQ-learned value functions speed up learning in the different settings over learning simply with sparse rewards (orange line *vs.* blue line). In all settings except Freeway, our method not only learns more quickly than sparse reward, but converges to a higher mean performance.

LAQ discovers stronger behavior than imitation learning when faced with undirected experience. An advantage of LAQ over other imitation-learning based methods such as BCO (Torabi et al., 2018a) and ILPO (Edwards et al., 2019) is LAQ's ability to learn from sub-optimal or undirected experience. To showcase this, we compare the performance of LAQ with behavior cloning (BC) with ground truth actions. Since BCO and ILPO recover ground truth actions to perform behavior cloning (BC), BC with ground truth actions serves as an upper bound on the performance of all methods in this class. Learning plots in Figure 4 shows the effectiveness of LAQ over BC and BC followed by fine-tuning with sparse rewards for environments where the experience is undirected (Maze2D, and GridWorld). For Freeway, the experience is fairly goal-directed, thus BC already works well. A similar trend can be seen in the higher Spearman's coefficient for LAQ *vs.* $V_{\text{one-act}}$ in Table 1. LAQ discovers stronger behavior than imitation learning when faced with undirected data.

LAQ is compatible with other advances in batch RL. Although LAQ uses the most basic Q-Learning as our offline value learning method, it is compatible with recent more advanced offline RL value-learning methods (such as CQL (Kumar et al., 2020) and BCQ (Fujimoto et al., 2019)). We validate this in the Maze2D environment, where we simply swap to using (discrete) BCQ with our latent actions. Figure 4 shows that LAQ with BCQ is the strongest method, outperforming ours with DQN and D3G on the Maze2D environment. Analysis of Spearman's correlations in Table 2 shows the same trend as before with latent actions: better than single actions, and clustering variants. Note also that use of BCQ leads to value functions with better Spearman's correlations than DQN.

Table 2: We report Spearman's correlation coefficients for value functions learned using either DQN or BCQ, against a value function learned offline using BCQ with ground-truth actions. The *Ground Truth Actions* column shows Spearman's correlation coefficients between two different runs of offline learning with ground-truth actions. See Section 5.1.

Environment	Single Action	Clustering	Clustering (Diff)	Latent Actions	Ground Truth Actions
2D Continuous Control (DQN)	0.664	0.431	0.312	**0.807**	0.765
2D Continuous Control (BCQ)	0.710	0.876	0.719	**0.927**	0.990

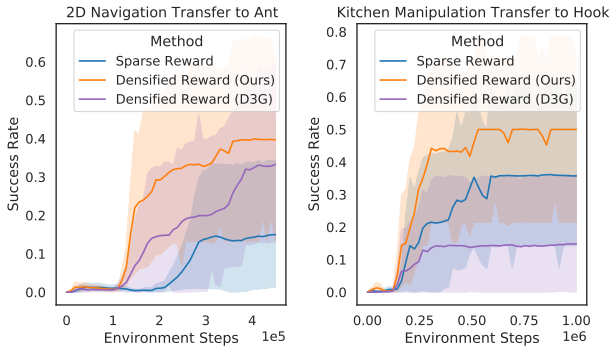

Figure 5: Learning curves for acquiring behavior with value functions transferred across embodiment. We compare LAQ densified RL *vs.* sparse RL and D3G densified RL. Results averaged over 5 seeds and show 95% confidence intervals.

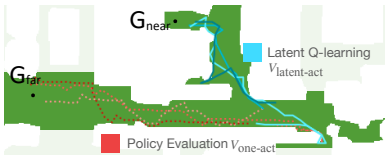

	Interaction Samples	SPL
$V_{\text{one-act}}$ (Chang et al., 2020)	0	0.53
$V_{\text{cluster-act}}$	0	0.57
$V_{\text{latent-act}}$	0	0.82
$V_{\text{inverse-act}}$ (Chang et al., 2020)	40K	0.95

Figure 6: Visualization of trajectories and SPL numbers in the 3D visual navigation environment.

LAQ value functions allow transfer across embodiments. Figure 5 shows learning plots of agents trained with cross-embodiment value functions. LAQ-densified rewards functions, speed-up learning and consistently guide to higher reward solutions than sparse task rewards, or D3G.

LAQ compares favorably to D3G. We compare LAQ and D3G (a competing state-only method) in different ways. D3G relies on generating potential future states. This is particularly challenging for image observations, and D3G doesn't show results with image observations. In contrast, LAQ maps state transitions to discrete actions, and hence works with image observations as our experiments show. Even in scenarios with low-dimensional state inputs, LAQ learns better value functions than D3G, as evidences by Spearman's correlations in Table 1, and learning plots in Figure 4 and Figure 5.

LAQ value functions can guide low-level controllers for zero-shot control: We report the SPL for 3D navigation using value functions combined with low-level controllers in Figure 6. We report the efficiency of behavior induced by LAQ learned value functions as measured by the SPL metric (Success weighted by inverse Path Length) from Anderson et al. (2018) (higher is better). The branching environment has two goal states, one optimal and one sub-optimal. The demonstrations there-in were specifically designed to emphasize the utility of knowing the intervening actions. Simple policy evaluation leads sub-optimal behavior (SPL of 0.53) and past work relied on using an inverse model to label actions (Chang et al., 2020) to derive better behavior. This inverse model itself required $40K$ interactions with the environment for training, and boosted the SPL to 0.95. LAQ is able to navigate to the optimal goal (w/ SPL 0.82) but without the $40K$ online interaction samples necessary to acquire the inverse model. It also performs better than clustering transitions, doing which achieves an SPL of 0.57. The improvement is borne out in visualizations in Figure 6. LAQ correctly learns to go to the nearer goal, even when the underlying experience came from a policy that preferred the further away goal.

6 Discussion

Our theoretical characterization and experiments in 5 representative environments showcase the possibility and potential of deriving goal-directed signal from undirected state-only experience. Here we discuss some scenarios which are fundamentally hard, and some avenues for future research.

Non-deterministic MDPs. Our theoretical result relies on a refinement where state-action transition probabilities are matched. However, the latent action mining procedure in LAQ results in determin-

istic actions. Thus, for non-deterministic MDPs (where executing the same action in the same state takes the agent to different next state), LAQ will be unable to achieve a strict refinement, leading to sub-optimal value functions. However, note that this limitation isn't specific to our method, but applies to *any* deterministic algorithm that seeks to learn from observation only data. We formalize this concept and provide a proof in Section A.2.

Constraining evaluation of $V(s)$ to withing its domain. LAQ learns a value function $V(s)$ over the set of states that were available in the experience dataset, and as such its estimates are only accurate within this set. In situations where the experience dataset doesn't span the entire state space, we may need to assess where the predictions of $V(s)$ are valid (otherwise densified RL may find a spuriously high-value region outside the valid domain of $V(s)$). We discuss a density based model solution we used for this problem in Section A.4.

Offline RL Validation. Validation (*e.g.* when to stop training) is a known issue in offline RL (Gulcehre et al., 2020). Like other offline RL methods, LAQ suffers from it too. LAQ's use of Q-learning makes it compatible to recent advances (Kumar et al., 2021) that tackle this validation problem.

7 Related Work

Our work focuses on batch (or offline) RL with state-only data using a latent-variable future prediction model. We survey works on batch RL, state-only learning, and future prediction.

Batch Reinforcement Learning. As the field of reinforcement learning has matured, batch RL (Lange et al., 2012; Levine et al., 2020) has gained attention as a component of practical systems. In recent times, Gulcehre et al. (2020) and Fu et al. (2020) propose datasets and experimental setups for studying offline RL problems. A large body of work examines solutions to the batch RL problem. Researchers have identified that *extrapolation error*, the phenomenon in which batch RL algorithms incorrectly estimate the value of states/actions not present in the training batch, is a major challenge, and have proposed methods to tackle it, *e.g.* BCQ (Fujimoto et al., 2019), BEAR (Kumar et al., 2019b), IRIS from (Mandlekar et al., 2020), and CQL (Kumar et al., 2020) among many others. In contrast to these model-free methods, Argenson & Dulac-Arnold (2021); Rajeswaran et al. (2019); Rafailov et al. (2020) learn a forward predictive model from the batch data and use it for model predictive control. These methods all approach the traditional batch RL problem, while we consider a different and harder setting in which the action labels are unavailable. Aforementioned advances in offline RL are complementary to our work. Offline value learning approaches (such as CQL and BCQ) can serve as a drop-in replacement for Q-learning in our pipeline and improve our results. In fact, our experiments with BCQ substantiate this.

State-only Learning. Some past works have explored different approaches for dealing with the lack of actions in offline RL when given *a) goal-directed* or *b) undirected* observation-only experience. In the former category of goal-directed experience, researchers use imitation learning-based techniques (Radosavovic et al., 2020; Torabi et al., 2018a; Edwards et al., 2019; Kumar et al., 2019a), or learn policies that match the distribution of visited states (Torabi et al., 2018b; 2019a;b), or use demonstrations to construct dense reward functions (Shao et al., 2020; Sermanet et al., 2017; Singh et al., 2019; Xie et al., 2018; Edwards & Jr., 2019). These methods make strong assumptions about the quality and goal-directed nature of the experience data, and suffer in performance when faced with low-quality or undirected experience. Our work falls in the second category and we tackle the problem when given undirected experience. Past work in this category employs Q-learning to learn optimal behavior from sub-optimal data (Chang et al., 2020; Song et al., 2020; Edwards et al., 2020). Chang et al. (2020) and Song et al. (2020) use domain specific insights. Edwards et al. (2020) rely on being able to generate the next state and only demonstrate results in environments with low-dimensional states. Instead, our work maps transition tuples to discrete latent actions and can thus easily work with high-dimensional observations such as RGB images.

Future Prediction Models. Past work from Oh et al. (2015); Agrawal et al. (2016); Finn et al. (2016) (among many others) has focused on building action conditioned forward models in pixel and latent spaces. Yet other work in computer vision studies video prediction problems (Xue et al., 2016; Castrejon et al., 2019). Given the uncertainty in future prediction, these past works have pursued variational (or latent variable) approaches to make better predictions. Our latent variable future model is inspired from these works, but we explore its applications in a novel context.

REFERENCES

Rishabh Agarwal, Dale Schuurmans, and Mohammad Norouzi. An optimistic perspective on offline reinforcement learning. In *International Conference on Machine Learning*, pp. 104–114. PMLR, 2020. 17, 18

Pulkit Agrawal, Ashvin V Nair, Pieter Abbeel, Jitendra Malik, and Sergey Levine. Learning to poke by poking: Experiential learning of intuitive physics. In *NeurIPS*, 2016. 9

Peter Anderson, Angel Chang, Devendra Singh Chaplot, Alexey Dosovitskiy, Saurabh Gupta, Vladlen Koltun, Jana Kosecka, Jitendra Malik, Roozbeh Mottaghi, Manolis Savva, and Amir Zamir. On evaluation of embodied navigation agents. *arXiv preprint arXiv:1807.06757*, 2018. 8

Arthur Argenson and Gabriel Dulac-Arnold. Model-based offline planning, 2021. 9

M. G. Bellemare, Y. Naddaf, J. Veness, and M. Bowling. The arcade learning environment: An evaluation platform for general agents. *Journal of Artificial Intelligence Research*, 47:253–279, jun 2013. 5

Christopher M Bishop. *Pattern recognition and machine learning*. springer, 2006. 4

Lluis Castrejon, Nicolas Ballas, and Aaron Courville. Improved conditional vrnns for video prediction. In *Proceedings of the IEEE/CVF International Conference on Computer Vision*, pp. 7608–7617, 2019. 9

Matthew Chang, Arjun Gupta, and Saurabh Gupta. Semantic visual navigation by watching youtube videos. In *NeurIPS*, 2020. 5, 7, 8, 9, 17, 18, 21

Ashley D. Edwards and Charles L. Isbell Jr. Perceptual values from observation. *CoRR*, abs/1905.07861, 2019. 9

Ashley D Edwards, Himanshu Sahni, Yannick Schroecker, and Charles L Isbell. Imitating latent policies from observation. In *ICML*, 2019. 5, 7, 9

Ashley D. Edwards, Himanshu Sahni, Rosanne Liu, Jane Hung, Ankit Jain, Rui Wang, Adrien Ecoffet, Thomas Miconi, Charles Isbell, and Jason Yosinski. Estimating $q(s, s')$ with deep deterministic dynamics gradients. In *ICML*, 2020. 5, 6, 9

Chelsea Finn, Ian Goodfellow, and Sergey Levine. Unsupervised learning for physical interaction through video prediction. *arXiv preprint arXiv:1605.07157*, 2016. 9

Justin Fu, Aviral Kumar, Ofir Nachum, George Tucker, and Sergey Levine. D4RL: Datasets for deep data-driven reinforcement learning. *arXiv preprint arXiv:2004.07219*, 2020. 5, 9, 17

Scott Fujimoto, David Meger, and Doina Precup. Off-policy deep reinforcement learning without exploration. In *ICML*, 2019. 5, 7, 9

Caglar Gulcehre, Ziyu Wang, Alexander Novikov, Tom Le Paine, Sergio Gómez Colmenarejo, Konrad Zolna, Rishabh Agarwal, Josh Merel, Daniel Mankowitz, Cosmin Paduraru, Gabriel Dulac-Arnold, Jerry Li, Mohammad Norouzi, Matt Hoffman, Ofir Nachum, George Tucker, Nicolas Heess, and Nando deFreitas. Rl unplugged: Benchmarks for offline reinforcement learning, 2020. 9

Matt Hoffman, Bobak Shahriari, John Aslanides, Gabriel Barth-Maron, Feryal Behbahani, Tamara Norman, Abbas Abdolmaleki, Albin Cassirer, Fan Yang, Kate Baumli, et al. Acme: A research framework for distributed reinforcement learning. *arXiv preprint arXiv:2006.00979*, 2020. 6

Ashish Kumar, Saurabh Gupta, and Jitendra Malik. Learning navigation subroutines by watching videos. In *CoRL*, 2019a. 9

Aviral Kumar, Justin Fu, Matthew Soh, George Tucker, and Sergey Levine. Stabilizing off-policy q-learning via bootstrapping error reduction. In *NeurIPS*, 2019b. 9

Aviral Kumar, Aurick Zhou, George Tucker, and Sergey Levine. Conservative q-learning for offline reinforcement learning. In *NeurIPS*, 2020. 5, 7, 9

Aviral Kumar, Anikait Singh, Stephen Tian, Chelsea Finn, and Sergey Levine. A workflow for offline model-free robotic reinforcement learning. In *CoRL*, 2021. 9

Sascha Lange, Thomas Gabel, and Martin Riedmiller. Batch reinforcement learning. In *Reinforcement learning*, pp. 45–73. Springer, 2012. 2, 9

Sergey Levine, Aviral Kumar, George Tucker, and Justin Fu. Offline reinforcement learning: Tutorial, review, and perspectives on open problems. *arXiv preprint arXiv:2005.01643*, 2020. 2, 9

Ajay Mandlekar, Fabio Ramos, Byron Boots, Silvio Savarese, Fei-Fei Li, Animesh Garg, and Dieter Fox. IRIS: implicit reinforcement without interaction at scale for learning control from offline robot manipulation data. In *ICRA*, 2020. 9

Volodymyr Mnih, Koray Kavukcuoglu, David Silver, Alex Graves, Ioannis Antonoglou, Daan Wierstra, and Martin Riedmiller. Playing atari with deep reinforcement learning. *arXiv preprint arXiv:1312.5602*, 2013. 4

Andrew Y. Ng, Daishi Harada, and Stuart J. Russell. Policy invariance under reward transformations: Theory and application to reward shaping. In *ICML*, pp. 278–287. Morgan Kaufmann, 1999. 5

Junhyuk Oh, Xiaoxiao Guo, Honglak Lee, Richard Lewis, and Satinder Singh. Action-conditional video prediction using deep networks in atari games. *arXiv preprint arXiv:1507.08750*, 2015. 9

Ilija Radosavovic, Xiaolong Wang, Lerrel Pinto, and Jitendra Malik. State-only imitation learning for dexterous manipulation. *CoRR*, abs/2004.04650, 2020. 9

Rafael Rafailov, Tianhe Yu, Aravind Rajeswaran, and Chelsea Finn. Offline reinforcement learning from images with latent space models. *CoRR*, abs/2012.11547, 2020. 9

Aravind Rajeswaran, Chelsea Finn, Sham Kakade, and Sergey Levine. Meta-learning with implicit gradients. *arXiv preprint arXiv:1909.04630*, 2019. 9

Manolis Savva, Abhishek Kadian, Oleksandr Maksymets, Yili Zhao, Erik Wijmans, Bhavana Jain, Julian Straub, Jia Liu, Vladlen Koltun, Jitendra Malik, Devi Parikh, and Dhruv Batra. Habitat: A platform for embodied AI research. In *ICCV*, 2019. 5, 17, 18

Pierre Sermanet, Kelvin Xu, and Sergey Levine. Unsupervised perceptual rewards for imitation learning. In *RSS*, 2017. 9

Lin Shao, Toki Migimatsu, Qiang Zhang, Karen Yang, and Jeannette Bohg. Concept2robot: Learning manipulation concepts from instructions and human demonstrations. In *RSS*, 2020. 9

Avi Singh, Larry Yang, Chelsea Finn, and Sergey Levine. End-to-end robotic reinforcement learning without reward engineering. In *RSS*, 2019. 9

Shuran Song, Andy Zeng, Johnny Lee, and Thomas Funkhouser. Grasping in the wild: Learning 6dof closed-loop grasping from low-cost demonstrations. *Robotics and Automation Letters*, 2020. 9

Richard S. Sutton and Andrew G. Barto. *Reinforcement Learning: An Introduction*. A Bradford Book, Cambridge, MA, USA, 2018. ISBN 0262039249. 2, 13

Faraz Torabi, Garrett Warnell, and Peter Stone. Behavioral cloning from observation. In *IJCAI*, 2018a. 5, 7, 9

Faraz Torabi, Garrett Warnell, and Peter Stone. Generative adversarial imitation from observation. *CoRR*, abs/1807.06158, 2018b. 9

Faraz Torabi, Garrett Warnell, and Peter Stone. Adversarial imitation learning from state-only demonstrations. In *AAMAS*, pp. 2229–2231. International Foundation for Autonomous Agents and Multiagent Systems, 2019a. 9

Faraz Torabi, Garrett Warnell, and Peter Stone. Imitation learning from video by leveraging proprioception. *arXiv preprint arXiv:1905.09335*, 2019b. 9

Christopher John Cornish Hellaby Watkins. Learning from delayed rewards. 1989. 2, 4, 14

Annie Xie, Avi Singh, Sergey Levine, and Chelsea Finn. Few-shot goal inference for visuomotor learning and planning. In *Conference on Robot Learning*, pp. 40–52. PMLR, 2018. 9

Tianfan Xue, Jiajun Wu, Katherine L Bouman, and William T Freeman. Visual dynamics: Probabilistic future frame synthesis via cross convolutional networks. *arXiv preprint arXiv:1607.02586*, 2016. 9

A APPENDIX

A.1 PROOFS

Proof. **Proof for Lemma 3.2.** We will start by showing that for any policy $\pi_{\hat{M}}$ on $\hat{M}$, there exists a policy π_M on M such that $V_{\hat{M}}^{\pi_{\hat{M}}}(s) = V_M^{\pi_M}(s)$, for all s.
To do this we need to introduce the idea of *fundamental actions*, which are classes of of actions which have the same state and reward transition distributions in a given state. If we have a fundamental action b, corresponding to some state and reward distributions, let $\alpha(b) \subseteq \mathbf{A}$ give the set of actions in $\mathbf{A}$ that have the matching state and reward distributions,

$$\underset{a \in \alpha(b)}{\forall} p(s', r|s, a) = p(s', r|s, \alpha(b)_1).$$

Similarly, let $\hat{\alpha}(b) \subseteq \hat{\mathbf{A}}$ give the set of actions in $\hat{\mathbf{A}}$ belonging to b. In any given state, there are at at most $\min(|\mathbf{A}|, |\hat{\mathbf{A}}|)$ fundamental actions for M and the union of all actions belonging to all fundamental actions gives the set of actions that make up the original action space. For our MDP let's denote $B(s)$ as the set of fundamental actions in the state s for M, and $\hat{B}(s)$ as the set of fundamental actions in the state s for $\hat{M}$. Let $\beta(s, a)$, and $\hat{\beta}(s, a)$ be a functions which return the fundamental action containing a in state s for M, and $\hat{M}$ respectively. This means,

$$\bigcup_{b \in B(s)} \alpha(b) = A, \underset{b \in B(s)}{\forall} \underset{b' \neq b}{\forall} \alpha(b) \cap \alpha(b') = \emptyset, \text{ and } \underset{a \in A, s}{\forall} \exists_{b \in B(s)} | a \in \alpha(b). \tag{1}$$

With this notation out of the way we can construct a policy $\pi_{\hat{M}}$ from π_M, which achieves the same value in $\hat{M}$ as π_M does in M. We do this by constructing $\pi_{\hat{M}}$ such that the probability distributions over each *fundamental action* is equivalent. We define this policy as

$$\pi_M(a|s) = \frac{1}{|\beta(s, a)|} \sum_{\hat{a} \in \hat{\beta}(s,a)} \pi_{\hat{M}}(\hat{a}|s)$$

Following Sutton & Barto (2018) we can define the value function for a given policy as

$$V_M^{\pi_M}(s) = \mathbb{E}_{\pi_M}[G_t | S_t = s]$$

$$V_M^{\pi_M}(s) = \sum_{a \in \mathbf{A}} \pi_M(a|s) \sum_{s', r} p(s', r|s, a) \big[r + \gamma V_M^{\pi_M}(s')\big]$$

From the properties in Eq. 1, we know a sum over action in each fundamental action will count each action exactly once, so we can write this sum as

$$V_M^{\pi_M}(s) = \sum_{b \in B(s)} \sum_{a \in \alpha(b)} \pi_M(a|s) \sum_{s', r} p(s', r|s, a) \big[r + \gamma V_M^{\pi_M}(s')\big] \tag{2}$$

substituting in the constructed policy we have

$$V_M^{\pi_M}(s) = \sum_{b \in B(s)} \sum_{a \in \alpha(b)} \left[\frac{1}{|\beta(s, a)|} \sum_{\hat{a} \in \hat{\beta}(s,a)} \pi_{\hat{M}}(\hat{a}|s)\right] \sum_{s', r} p(s', r|s, a) \big[r + \gamma V_M^{\pi_M}(s')\big]$$

since the third sum is over $\hat{\beta}(s, a)$ with $a \in \alpha(b)$, we can rewrite this sum as over $\hat{a} \in \hat{\alpha(b)}$, giving

$$V_M^{\pi_M}(s) = \sum_{b \in B(s)} \sum_{a \in \alpha(b)} \left[\frac{1}{|\beta(s, a)|} \sum_{\hat{a} \in \hat{\alpha}(b)} \pi_{\hat{M}}(\hat{a}|s)\right] \sum_{s', r} p(s', r|s, a) \big[r + \gamma V_M^{\pi_M}(s')\big].$$

For the final sum, from the definition of fundamental actions, we know $p(s', r|s, a) = p(s', r|s, \alpha(b)_1) = \hat{p}(s', r|s, \hat{\alpha}(b)_1)$, so we can rewrite that term as

$$\sum_{s', r} \hat{p}(s', r|s, \hat{\alpha}(b)_1) \big[r + \gamma V_M^{\pi_M}(s')\big].$$

Crucially, in the second sum (over $a \in \alpha(b)$), $\hat{B}(s,a)$ is the same for all $a \in \alpha(b)$, so the term in brackets can be treated as a constant. Similarly, Since $|B(s,a)| = |b|$ we can simplify the second sum leaving

$$V_M^{\pi_M}(s) = \sum_{b \in B(s)} \sum_{\hat{a} \in \hat{\alpha}(b)} \pi_{\hat{M}}(\hat{a}|s) \sum_{s',r} \hat{p}(s',r|s,\hat{\alpha}(b)_1)\big[r + \gamma V_M^{\pi_M}(s')\big].$$

This gives the definition of $V_{\hat{M}}^{\pi_{\hat{M}}}(s)$ using the same decomposition as equation Eq. 2, meaning

$$V_M^{\pi_M}(s) = V_{\hat{M}}^{\pi_{\hat{M}}}(s).$$

□

Proof for Theorem 3.1. Under the new MDP $\hat{M}$, Q-learning will learn the same optimal value function value function as learned under MDP M, *i.e.* $\forall_s V_{\hat{M}}^*(s) = V_M^*(s)$.

Proof. This follows from Lemma 3.2 by contradiction. Assume there is a state s' where $V_{\hat{M}}^*(s) \neq V_M^*(s)$. Two cases must be considered. First, is the case where $V_{\hat{M}}^*(s) > V_M^*(s)$. We will notate the optimal policy in $\hat{M}$ as $\tilde{\pi}_{\hat{M}}^*$ (*i.e.* $V_{\hat{M}}^* = V_{\hat{M}}^{\tilde{\pi}_{\hat{M}}^*}$) and the optimal policy in M as π_M^*. We know there must exist a policy $\tilde{\pi}_M^*$ such that $V_M^{\tilde{\pi}_M^*}(s) = V_{\hat{M}}^{\tilde{\pi}_{\hat{M}}^*}(s)$ from Lemma 3.2. We arrive at a contradiction because $V_M^{\tilde{\pi}_M^*}(s) > V_M^{\pi_M^*}(s)$, so π_M^* could not have been the optimal policy on M. The other direction follows a symmetric argument. If $V_{\hat{M}}^{\tilde{\pi}_{\hat{M}}^*}(s) < V_M^{\pi_M^*}(s)$, we know there must be a policy $\pi_{\hat{M}}^*$ in $\hat{M}$ such that $V_M^{\pi_M^*}(s) = V_{\hat{M}}^{\pi_{\hat{M}}^*}(s)$. This implies $V_{\hat{M}}^{\pi_{\hat{M}}^*}(s) > V_{\hat{M}}^{\tilde{\pi}_{\hat{M}}^*}(s)$, meaning that $\tilde{\pi}_{\hat{M}}^*$ could not have been the optimal policy. Since Q-learning is known to converge to the optimal value function Watkins (1989), Q-learning on $\hat{M}$ will converge to the original value function V_M^*. □

A.2 STATE ONLY LEARNING FROM STOCHASTIC MDPS

Here we will briefly prove that problem of deducing the optimal value function of an MDP M, from some state-only experience dataset D, cannot be solved in general for non-deterministic MDPs. We notate $\mathbb{D}$ as the space of all *complete* state-only datasets, and $\mathbb{V}$ as the space of all value functions. By *complete* state-only dataset, we mean datasets in which all possible transition triples (s, s', r) appear. Note that exactly one complete dataset exists for each MDP. We denote D_M as the complete dataset corresponding to an MDM M.

In short, the idea is to construct a single state-only dataset which ambiguously could have been produced from two different MDPs which have different optimal value functions. Since no function deterministic function can model two outputs from the same input, no such function can exist.

Theorem A.1. *For any function $f : \mathbb{D} \to \mathbb{V}$ which maps from the set of of state-only datasets, $\mathbb{D}$, to a set of value functions. There exists some MDP M, with corresponding dataset D_M such that $f(D) \neq V^*_M$.*

$$\nexists f \mid \forall_M f(D_M) = V^*_M$$

Proof. We proceed by contradiction, assume any $f : \mathbb{D} \to \mathbb{V}$ such that

$$\forall_M f(D_M) = V^*_M.$$

If we can construct M_1 and M_2 such that $V^*_{M_1} \neq V^*_2$, and D such that $D = D_{M_1} = D_{M_2}$, then f cannot produce the correct value function for $f(D)$ in all cases, from the definition of a function. We will now show a very simple construction which exhibits this property. Consider an MDP M_1, with 3 states, s_1, s_2, s_t, and 2 actions a_1, a_2. s_t is terminal, and gives reward 1, other states give reward 0. The transition dynamics of the two actions are given below.

Table: a_1 transitions for M_1

	s_1	s_2	s_t
s_1	0	1	0
s_2	0	0	1

Table: a_2 transitions for M_1

	s_1	s_2	s_t
s_1	0	0	1
s_2	1	0	0

For simplicity, assume M_1 has a discount factor of 0.9. This means $V^*(s_1) = V^*(s_2) = 1$.

We define M_2 as identical to M_1, only with stochastic transitions.

Table: a_1 transitions for M_2

	s_1	s_2	s_t
s_1	0	1	0
s_2	0	0	1

Table: a_2 transitions for M_2

	s_1	s_2	s_t
s_1		0.9	0.1
s_2	1	0	0

In this MDP, with a discount factor of 0.9, $V^*(s_2) = 1$, but $V^*(s_1) = 0.1 + 0.9 * 0.9 = 0.91$.

Since both M_1 and M_2 share the same states, actions, and possible transitions, $D_{M_1} = D_{M_2}$. So we have satisfied our condition that $D = D_{M_1} = D_{M_2}$, and $V^*_{M_1} \neq V^* M_2$. Thus, no f can model the value functions for both MDPs in general. □

A.3 GRID WORLD BEHAVIOR *vs.* PURITY

Figure S7 plots the MSE in value function and the proportion of states with correct implied actions as a function of the noise in the action labels.

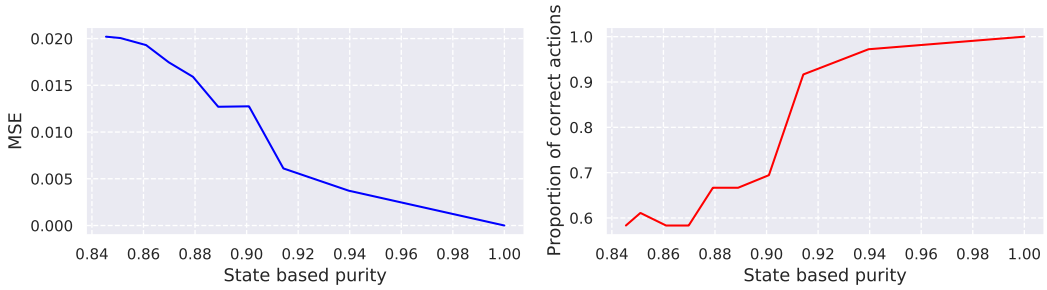

Figure S7: We plot correctness of value function estimate and behavior as a function of state-based purity of the intervening actions used for Q-learning. Left plot shows the mean squared error (lower is better) between the obtained value function and the optimal value function. Right plot shows fraction of states in which the learned value function induces the optimal action (higher is better). Both value function and behaviors become worse as state-based purity decreases. See Section 3.2.

A.4 ENVIRONMENT DETAILS

2D Grid World. We use the environment and data from Section 3.2. We use the (x, y) coordinates as our state for this environment. We use a multi-layer perceptron for f_θ and L2 loss for l.

2D Continuous Control Navigation. We use the Maze2D data from D4RL Fu et al. (2020). Observation space here is (x, y, v_x, v_y) *i.e.* location and velocity of the agent, and action space is force along x and y directions. We use a frame skip of 3. We use a multi-layer perceptron for f_θ and L2 loss for l. In the embodiment transfer variant, we swap the agent for a 4-legged ant, also from D4RL. The ant embodiment is far more challenging to control, with an 8-d action space and 29-d observation space.

Atari Game. We work with Freeway. We generated our own data using the protocol described in Agarwal et al. (2020). We turned off sticky actions and store frames both at the default resolution (84×84) and full resolution (224×224). Other settings are same as is typical: stack last 4 frames to represent the observations, and use frame-skip of 4. We use a convolutional encoder-decoder model for f_θ and predict raw future observations. We use L2 distance in the pixel space as our loss function l.

3D Visual Navigation. We work with the branching environment from Chang et al. (2020) in the AI Habitat Simulator Savva et al. (2019), and use the provided dataset of first-person trajectories as our pre-recorded experience dataset. Following Chang et al. (2020), we employ low-level controllers for deriving behaviors from the learned value functions. We use a convolutional encoder-decoder for f_θ, and L2 loss in pixel space as l.

Kitchen Manipulation. In this task a 9-DOF Franka arm can interact with several different objects physically simulated kitchen. The observations are 24-d, containing the end-effector position and state of various objects in the environment (microwave door angle, kettle position, etc.). The action space represents the 9-d joint velocity. In cross-embodiment experiments we replace the Franka arm with a hook. The observation space remains the same while the action space becomes 3-d position control.

For experiments in kitchen manipulation, we add an additional component to the reward computation to incentivize behavior to remain within the region of the state space covered by the demonstrations (where the learned value function is in-distribution). To do this, we build a density model over the end effector position using a 2 component Gaussian mixture model. If a state s has a less than 1% probability according to the GMM density model, then we assign $V(s) = 0$, for the update described in Section 5.2. We apply this shaping to both ours and D3G in Figure 4. We give sparse reward the same benefit of this shaping by giving reward -1 outside of the GMM distribution, and 0 inside. Sparse task reward remains the same.

For all environments, we throw out the provided action labels when learning our models.

A.5 DATA COLLECTION

2D Grid World. The setting for this experiment is a 6×6 grid with 8 actions, corresponding to moving in the 4 cardinal directions and 4 diagonal directions. The agent starts in the top left (0,0), and gets reward 0 everywhere, except for in the bottom right, (5,5). Reaching the bottom right gives the agent reward 1 and terminates the episode. In the starting square (0,0), the agent has probability 0.5 of moving right, and probability 0.5 of moving down. When the agent is on the top or bottom edge of the maze (row = 0 or row = 5) it moves right with probability 0.9, and takes a random action with probability 0.1. When it is on the left or right edge of the grid (column = 0 or column = 5), it moves down with probability 0.9 and takes a random action with probability 0.1. Otherwise, it is in the interior of the grid, where it takes an action away from the goal (randomly chosen from: up, left, or up-left) with probability 0.9, and one of the remaining actions otherwise (randomly chosen from: down, right, down-right, up-right, down-left). This policy is rolled out for 20,000 policies to generate the data for methods described in main paper Section 3.2 and Figure 1.

Atari Game. Data for the Freeway environment had to be additionally collected, as native high resolution resolution images of the episodes from Agarwal et al. (2020) are not readily available. For this, we re-generated the data using the protocal described in Agarwal et al. (2020), without sticky actions. Then, the high resolution data was collected by taking the action sequences from the re-generated dataset and executing them in an emulator, while storing the native resolution images. Because we re-generated the data without sticky actions, the high resolution episodes are perfect recreations of the low resolution episodes.

Visual Navigation. The data used for the visual navigation experiment was generated using the same protocol as Chang et al. (2020). Agents are tasked to reach one of two goals (G_{near} and G_{far}) in a visually realistic simulator Savva et al. (2019). Navigating to G_{near} is the optimal path as it is nearer to the agent's starting location.

The dataset contains 3 types of trajectories, T_1, T_2, and T_3, representing 50%, 49.5%, and 0.5% of the trajectories in the dataset respectively . T_1 takes a sub-optimal path to G_{near}, T_3 takes the optimal path to G_{near}, and T_2 navigates to G_{far}.

2D Continuous Control (Maze2D) We use the *Maze2D* dataset from D4RL as is.

Kitchen Manipulation. The data used for the Kitchen Manipulation environment comes from the *partial* version of the D4RL FrankaKitchen dataset. To facilitate cross-embodiment transfer we convert the state representation to contain end-effector location instead of joint angles.

A.6 LATENT ACTION QUALITY

We first measure the effectiveness of our latent action mining process by judging the extent to which the induced latent actions are a refinement of the original actions. We measure this using the *state-conditioned purity* of the partition induced by the learned latent actions. We approximate this by measuring the validation accuracy of a function g that is trained to map the high-dimensional state (or observation) s, and the associated latent action $\hat{a}$ to the actual ground truth action a.

Table S3 reports the purity (and MSE for continuous action environment) obtained by our proposed future prediction method. For reference, we also report the purity obtained when using *single action* that maps all samples into a single cluster, and 2 *clustering* methods that cluster either concatenation of the two observations *i.e.* $[o_{t+1}; o_t]$, or the difference between the two observations *i.e.* $[o_{t+1} - o_t]$. We use 8 latent actions for all environments except the FrankaKitchen environment for which we use 64 because of its richer underlying action space.

In general, our forward models are effective at generating a latent action space that is a state-conditioned refinement of the original action space. This is indicated by the improvement in state-conditioned purity values over using a single action or naive clustering. For the 2D Grid World and 2D Continuous Navigation, clustering in the correct space (state difference *vs.* state concatenation) works well as expected. But our future prediction model, which directly predicts s_{t+1} and doesn't use any domain specific choices, is able to outperform the corresponding clustering method. We also observe large improvements over all baselines for the challenging case of environments with high-dimensional state representations: Freeway and 3D Visual Navigation.

Table S3: We report the state-conditioned action purity (higher is better, MSE for continuous action case where lower is better), of latent actions for different approaches: single action, clustering concatenated observations, clustering difference in observations, and the proposed future prediction models from Section 4.1. We note the utility of the future prediction model for the challenging case of Freeway and 3D Visual Navigation environments. See Section A.6 for a full discussion.

Environment	**Observation Space**	**Action Space**	**Purity Metric**	**Single Action**	**Clustering** $[o_t, o_{t+1}]$	**Clustering** $[o_{t+1} - o_t]$	**Future Prediction**
2D Grid World	xy location	Discrete, 8	Purity (↑)	0.827	0.851	**1.000**	0.998
Freeway	210×160 image	Discrete, 3	Purity (↑)	0.753	0.778	0.773	**0.907**
3D Visual Navigation (Branching)	224×224 image	Discrete, 3	Purity (↑)	0.783	0.839	0.859	**0.928**
2D Continuous Control	xy loc. & vel	Continuous, 2	MSE (↓)	2.207	2.188	**0.325**	0.905
Kitchen Manipulation	24-d State	Continuous, 8	MSE (↓)	0.015	0.015	0.015	**0.014**

A.7 Analysis of Learned Latent Actions

We analyze the latent actions learned for the Freeway environment.

We visualize our future prediction model's predictions for the Freeway environment in Figure S8. In line with our expectations, the one action future prediction model and the latent action future prediction model are both able to reconstruct the background and the vehicles perfectly. At the same time, the one action future prediction model fails to reconstruct the agent accurately, whereas the latent action future prediction model is able to reconstruct the agent almost perfectly. This provides evidence for the effectiveness of our proposed latent action mining approach at discovering pure action groundings.

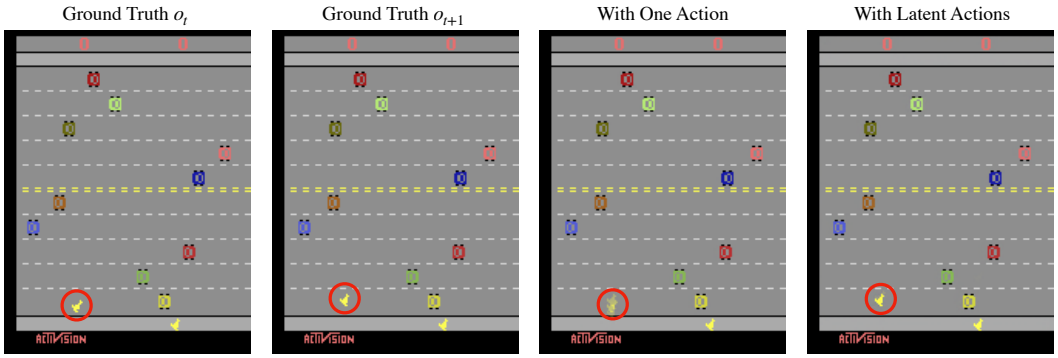

Figure S8: We visualize the Freeway future prediction models' reconstructions for o_{t+1}. From left to right, the ground truth o_t, the ground truth o_{t+1}, the reconstruction for o_{t+1} by the future prediction model with one action, the reconstruction for o_{t+1} by the future prediction model with latent actions. The agent is circled in each image.

Furthermore, we visualize the learned latent actions for Freeway in Figure S9. In Freeway, the agent can only move along the y-axis, and consequently, the environment action space only has three actions: move up, move down, and no-op. This means that the agent's y-displacement between the current frame and the previous frame directly corresponds to the ground truth action taken. In this visualization, we visualize the the chosen latent action (by color: blue, orange, or green) as a function of the agent's y-position in the current frame (x-axis) and the y-displacement relative to the previous frame (y-axis). Note that as mentioned in the paper, we learn the value functions over the top three most dominant actions to stabilize training; for this reason, the visualization only consists of three latent actions.

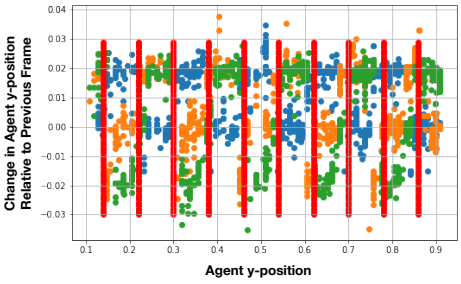

Figure S9: Visualization of the latent actions learned in Freeway. X-axis is the agent's y-position, y-axis is the displacement of the agent (which is indicative of ground truth action).

Within each vertical region marked by the red bars, we see that the latent actions are split into distinct clusters based on the agent's y-displacement. Because the agent's y-displacement directly corresponds to the ground truth action taken, this indicates that given the agent's y-position, the learned latent actions encode information about the ground truth action. Hence, we qualitatively confirm that the state-based purity of the latent actions is high.

A.8 VALUE FUNCTION DETAILS

Value Function Model Selection The numbers reported in Table 1 are the 95th percentile Spearman's correlation coefficients over the course of training. If training is stable and converges, this corresponds to taking the final value, and in the case that training is not stable and diverges, this acts as a form of early stopping. We take the 95th percentile as opposed to the maximum to eliminate outliers.

Below we present visualizations of value functions learned from LAQ.

Freeway. We visualize the value functions learned using our latent actions for Freeway. Figure S10 plots the values over the course of an episode. In Freeway, the agent has to move vertically up and down the screen to cross a busy freeway, receiving reward when it successfully gets to the other side. In a single episode, the agent can cross the freeway multiple times; each time the agent makes it to the other side, the agent's location is reset to the original starting location, allowing the agent to attempt to cross the freeway once again. For this reason, we see the value increase as the agent gets closer to the other side of the road, and then drop as soon as its position resets to the starting location. As evident, the peaks of the learned value function correspond highly to the environment reward.

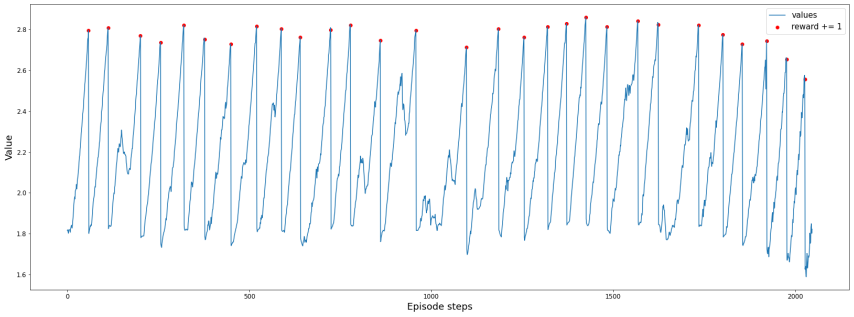

Figure S10: We visualize the value predicted by our learned value function over the course of one episode of Freeway. The red points correspond to when the agent receives a reward from the environment.

3D Visual Navigation. Figure S11 visualizes the learned value map in the 3D Visual Navigation branching environment from Chang et al. (2020). As depicted in Figure 6, there are two goals: G_{near} and G_{far}. The figure on the right illustrates that the value function learned by utilizing our latent actions correctly assigns high value to the regions surrounding the two goal locations, and low value elsewhere. Additionally, we learn the value functions with DQN using a dataset obtained by using a sub-optimal policy which prefers to go to the goal further away rather than the goal close by. Despite this sub-optimality, the learned value function correctly assigns a higher value to the nearby goal than the goal which is further away.

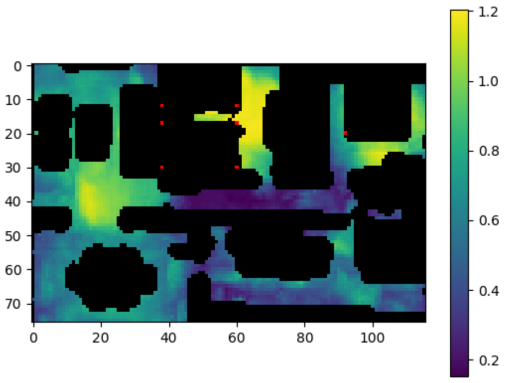

Figure S11: Visualization of the learned value function for 2D Continuous Control.

2D Continuous Control. Figure S12 shows a visualization of the value function learned using latent actions for the 2D Continuous Control environment. While the observation space of this environment is (x, y, v_x, v_y) *i.e.* location and velocity of the agent, we produce this visualization over just the location of the agent. Based on just the location of the agent, the optimal value function would be a monotonically decreasing function as the distance from the goal location increases. In this particular environment, the goal of the agent is to get to the top-right corner of the maze. The visualization shows that the learned value function produces high values around this goal region at the top-right corner of the maze, and gradually lower values the farther away you go. This figure visually is in line with our quantitative results in Table 1 which show that the value function learned using latent actions in the 2D Continuous Control environment highly correlates to that learned using ground truth actions.

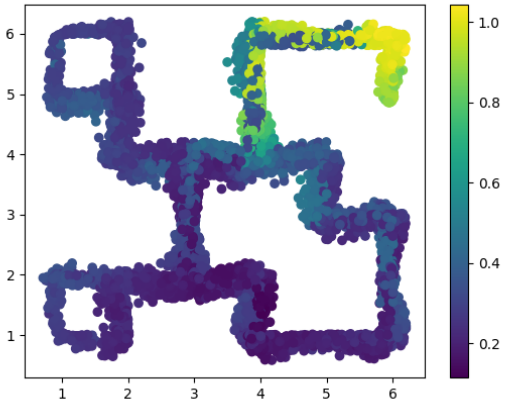

Figure S12: Visualization of the learned value function for 2D Continuous Control.

Kitchen Manipulation. We visualize the values as a function of both the angle that the microwave door makes with respect to its starting state as well as the distance between the end-effector and the microwave door handle in Figure S13. The task here is to open the microwave door: the agent receives a binary reward when the angle that the microwave door makes with respect to its starting state (i.e. closed microwave door) is above a threshold (approx. 0.7 radians), and zero otherwise. As expected, we see that the predicted value of a state increases as the angle of the microwave door increases. The end-effector position does not start out at the microwave door handle, but rather is initialized a fixed distance away from the handle. As a result, the agent must first move the end-effector to the microwave door handle, before interacting with the door handle to open it. In addition to this, we hypothesize that as the distance between the end-effector and the microwave door handle decreases, the predicted value should increase. While not as obvious as the relation between the microwave door angle and the value, we see some indication that as the distance between the end-effector and the microwave door handle decreases, the value increases.

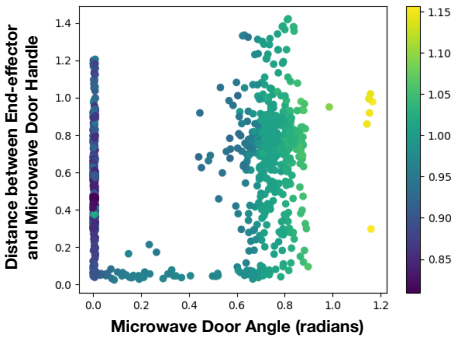

Figure S13: Visualization of the learned value function in Kitchen Manipulation. The x-axis is the microwave angle in radians, the y-axis is the distance between the end-effector and the microwave door handle, with the colors corresponding to the magnitude of the values.